Biochimica et Biophysica Acta 1803 (2010) 275–287

Contents lists available at ScienceDirect

Biochimica et Biophysica Acta

journal homepage: www.elsevier.com/locate/bbamcr

Protein kinase A regulation of $P2X_4$ receptors: Requirement for a specific motif in the C-terminus

David A. Brown, David I. Yule *

Department of Pharmacology and Physiology, School of Medicine and Dentistry, University of Rochester Medical Center, 601 Elmwood Avenue, Rochester NY 14642, USA

ARTICLE INFO

Article history:
Received 16 July 2009
Received in revised form 10 December 2009
Accepted 11 December 2009
Available online 21 December 2009

Keywords:
Protein kinase A (PKA)
Calcium signaling
P2X
Purinergic receptor
$P2X_4R$
Endocytosis
Intracellular calcium

ABSTRACT

The P2X purinergic receptor sub-family of ligand-gated ion channels are subject to protein kinase modulation. We have previously demonstrated that $P2X_4R$ signaling can be positively regulated by increasing intracellular cAMP levels. The molecular mechanism underlying this effect was, however, unknown. The present study initially addressed whether protein kinase A (PKA) activation was required. Subsequently a mutational approach was utilized to determine which region of the receptor was required for this potentiation. In both DT-40 3KO and HEK-293 cells transiently expressing $P2X_4R$, forskolin treatment enhanced ATP-mediated signaling. Specific PKA inhibitors prevented the forskolin-induced enhancement of ATP-mediated inward currents in $P2X_4R$ expressing HEK-293 cells. To define which region of the $P2X_4R$ was required for the potentiation, mutations were generated in the cytoplasmic C-terminal tail. It was determined that a limited region of the C-terminus, consisting of a non-canonical tyrosine based sorting motif, was required for the effects of PKA. Of note, this region does not harbor any recognizable PKA phosphorylation motifs, and no direct phosphorylation of $P2X_4R$ was detected, suggesting that PKA phosphorylation of an accessory protein interacts with the endocytosis motif in the C-terminus of the $P2X_4R$. In support of this notion, using Total Internal Reflection Fluorescence Microscopy (TIRF) $P2X_4$-EGFP was shown to accumulate at/near the plasma membrane following forskolin treatment. In addition, disrupting the endocytosis machinery using a dominant-negative dynamin construct also prevented the PKA-mediated enhancement of ATP-stimulated Ca^{2+} signals. Our results are consistent with a novel mechanism of P2XR regulation, whereby PKA activity, without directly phosphorylating $P2X_4R$, markedly enhances ATP-stimulated $P2X_4R$ currents and hence cytosolic Ca^{2+} signals. This may occur at least in part, by altering the trafficking of a population of $P2X_4R$ present at the plasma membrane.

1. Introduction

Extracellular adenosine triphosphate (ATP) can act as a signaling molecule by activating cell surface P2Y and P2X purinoreceptors [1]. Intracellular Ca^{2+} ($[Ca^{2+}]_i$) changes can be initiated by activation of Gαq-coupled P2Y receptor (P2YR) or as a result of P2X receptor (P2XR) activation. In contrast to P2YR, these receptors are non-selective Ca^{2+} permeable cation channels [2]. All P2XR are activated by ATP, but not by UTP [2,3]. To date there have been seven genes identified which code for P2XR ($P2X_1R$–$P2X_7R$). These proteins range in size from 388 to 595 amino acids (rat $P2X_4R$ and $P2X_7R$, respectively) and the sequences are most divergent in the C-terminus [2].

The predicted membrane topology of P2XR differs from other members of the ligand-gated channel super family. The generally accepted structural model proposes two transmembrane spanning domains with a large extracellular region containing the agonist binding site [4,5]. Both the N- and C-termini project into the cytosol. The functional P2XR channel is thought to be formed by the multimerization of three P2X subunits [6]. In turn, ATP is proposed to bind in an inter-molecular pocket formed between adjacent subunits coordinated by three conserved lysine residues near the extracellular ends of the transmembrane spanning domains [2,7]. This structural model has been largely based on extensive mutagenesis and structure–function studies. Notably, however, a majority of these anticipated features have been confirmed by a recent study in which the crystal structure of a substantial portion of the Zebra fish $P2X_4R$ in the closed state at 3.5 Å resolution was solved [8,9]. Compounding P2XR signaling complexity, there is also evidence that many P2XR subtypes can form functional heteromeric channels [10–14].

P2XR have been shown to be regulated by both protein kinase A (PKA) and protein kinase C (PKC) activation, suggesting they might be substrates for phosphorylation [15–18]. Previously our lab has

Abbreviations: ATP, adenosine 5′-triphosphate; cAMP, adenosine 3′,5′-cyclic monophosphate; PKA, protein kinase A; P2YR, P2Y receptor(s); P2XR, P2X receptor(s); $[Ca^{2+}]_i$, intracellular calcium concentration; $InsP_3R$, inositol 1,4,5-trisphosphate receptors; PM, plasma membrane; TIRF, Total Internal Reflection Fluorescence Microscopy

* Corresponding author. Tel.: +1 585 275 6128; fax: +1 585 273 2652.
E-mail address: David_Yule@urmc.rochester.edu (D.I. Yule).

0167-4889/$ – see front matter © 2009 Elsevier B.V. All rights reserved.
doi:10.1016/j.bbamcr.2009.12.002

demonstrated that $P2X_4R$ but not $P2X_7R$ signaling could be augmented by increasing intracellular cAMP levels [19]. The molecular mechanism was unclear at that time because cAMP acts on multiple effectors, including PKA and exchange proteins directly activated by cAMP (EPAC) [20,21]. Conceptually, PKA activation could directly phosphorylate $P2X_4R$ or alternatively might act indirectly by phosphorylation of an accessory protein. EPAC activation has been shown to activate the monomeric G protein Rap1, which can in turn lead to activation of downstream signaling events [20,21].

A principal goal of the present study therefore was to investigate the mechanism underlying cAMP-mediated enhancement of $P2X_4R$ signaling. The experiments in this study suggest a novel PKA-dependent mechanism, which does not involve direct phosphorylation of the $P2X_4R$. Nevertheless, we demonstrate that a limited region in the $P2X_4R$ C-terminus is required for the action of PKA. This region contains a non-canonical tyrosine based sorting motif, previously shown to be involved in the retrieval of the receptor from the plasma membrane (PM) via endocytosis. Our data support the notion that PKA phosphorylation alters trafficking by modulating endocytosis of $P2X_4R$ such that more functional receptors are present at the plasma membrane leading to enhanced current and augmented cytosolic Ca^{2+} signaling.

2. Materials and methods

2.1. PCR and primers

Primers for all constructs were from Integrated DNA Technologies (Coralville, IA). PCR reactions were performed as previously described using standard reagents from Invitrogen (Carlsbad, CA) [19]. The primer sequences are shown in Table 1.

2.2. Creation of P2XR constructs

Rat $P2X_4R$ cDNA was amplified by PCR to generate $P2X_4$-EGFP, $P2X_4$-Δ384-EGFP, $P2X_4$-Δ378-EGFP, and $P2X_4$-AAA-EGFP. HindIII and SalI restriction sites were incorporated into the oligonucleotides used for PCR amplification (shown in bold, Table 1). The PCR products were restriction enzyme digested and ligated into pEGFP-N3 at the HindIII and SalI sites (BD Biosciences Clontech, San Jose, CA). All constructs, which were verified by sequencing resulted in fusion proteins with EGFP at the C-terminus of the rat $P2X_4R$. Human $P2X_1R$ cDNA (kindly provided by R.A. North, University of Manchester, UK) was amplified by PCR to generate $P2X_4$-C-$P2X_1$-EGFP. AclI and SalI restriction sites were incorporated into the oligonucleotides used for PCR amplification (shown in bold, Table 1). The PCR products were digested with restriction enzyme and ligated into $P2X_4$-EGFP at the AclI and SalI sites. This construct, creates a chimeric $P2X_4R$ with the C-terminus of $P2X_1R$ which is C-terminally tagged with EGFP. Rat $P2X_4$-AAA-EGFP cDNA was amplified by PCR to generate $P2X_4$-AAA (untagged). HindIII and XhoI restriction sites were incorporated into the oligonucleotides used for PCR amplification (shown in bold, Table 1). The PCR product, following digestion was ligated into pCDNA3.1+ at the HindIII and XhoII sites (Invitrogen, Carlsbad, CA).

2.3. Transfection of DT-40 3KO/HEK-293 cells

Rat $P2X_4R$ constructs ($P2X_4$-EGFP, $P2X_4$-C-$P2X_1$-EGFP, $P2X_4$-Δ384-EGFP, $P2X_4$-Δ378-EGFP, and $P2X_4$-AAA-EGFP) were transiently transfected into DT-40 3KO cells using a Nucleofector System (Amaxa, Gaithersburg, MD) following the manufacturer's instructions. Specifically, 5×10^6 cells were resuspended in 100 μL of Cell-line Nucleofector Kit T solution and were transfected with 5 μg of the P2XR cDNA using Nucleofector program B-23. Experiments were performed 24 h after transfection. DT-40 3KO stable $P2X_4R$ expressing cells were transiently co-transfected with either 5 μg of empty vector (Mock) and 1 μg of pHcRed 1-N1 (red fluorescent protein for visualization of positively transfected cells) or 5 μg rat dynamin K44A (kindly provided by Dr. Patricia Hinkle, University of Rochester) and 1 μg of pHcRed 1-N1 using the procedure above.

$P2X_4R$ constructs were transiently transfected into HEK-293 cells using Lipofectamine 2000 (Invitrogen, Carlsbad, CA) as described previously [19,22]. Native P2XR constructs (non-EGFP tagged) were co-transfected with 100 ng of pHcRed 1-N1 cDNA per well.

2.4. Creation of stable $P2X_4R$-expressing DT-40 3KO and HEK-293 cells

NruI-digested plasmid (rat $P2X_4R$ in pcDNA3.1t) was introduced into DT-40 3KO cells by nucleofection using program B-23 and solution T as per the manufacturer's instructions (Amaxa, Gaithersburg, MD) to create the DT-40 3KO $P2X_4R$ stable cell line. After nucleofection, the cells were incubated in growth medium for 24 h prior to dilution in selection medium containing 2 mg/mL Geneticin (Invitrogen, Carlsbad, CA). Wells exhibiting growth after the 7 day selection period were picked for expansion. HEK-293 cells stably expressing EGFP- tagged $P2X_4R$ were generated using Flp-recombinase mediated integration. $P2X_4$-EGFP (rat $P2X_4R$ in pEGFP-N3) was digested in two steps with HindIII and NotI. This product was ligated into pcDNA5/FRT (Invitrogen, Carlsbad, CA) at these sites. Flp-In 293 cells (Invitrogen, Carlsbad, CA) which harbor a single FRT site were co-transfected with a 1:9 DNA ratio of $P2X_4$-EGFP in pcDNA5/FRT vector to pOG44 vector using Lipofectamine 2000 reagent. After 48 h, expressing cells were selected with hygromycin B (200 μg/mL). $P2X_4R$ expression was confirmed in hygromycin B-resistant colonies by the presence of EGFP fluorescence and through tests of $P2X_4R$ function as described.

2.5. Digital imaging of intracellular Ca^{2+}

DT-40 3KO cells were used as a null background for P2XR [22]. These cells lack all three (3KO) inositol 1,4,5-trisphosphate receptors ($InsP_3R$) and thus negate any possible Ca^{2+} response as a consequence of P2YR activation. DT-40 3KO cells were kindly provided by Dr. Kurosaki (Kansai Medical University, Japan) [23] and maintained as previously described [24–27]. DT-40 3KO cells were loaded with

Table 1
Oligonucleotide primers used to create $P2X_4R$ constructs. Sequences of the primers used to generate $P2X_4R$ mutations are shown. Note that restriction enzyme sites are highlighted in bold text.

	Forward Primer	Reverse Primer
P2X4-EG FP	GACGGC**AAGCTT**ATGGCGGGCTGCTGCTCCGTGCTCGGGTCC	TAGTTG**GTCGAC**CTGGTTCATCTCCCCCGAAAGACCCTG
P2X4-C-P2XI-EGFP	GACGGC**AACGTT**GGCTCTGGAATTGGCATCTTTGGGGTGGCC	TAGTTG**GTCGAC**GGATGTCCTCATGTTCTCCTGCAGGCCCAG
P2X4-Δ384-EGFP	GACGGC**AAGCTT**ATGGCGGGCTGCTGCTCCGTGCTCGGGTCC	TCA**GTCGAC**CGAAAGACCCTGCTCGTAGTCTTCCACATA
P2X4-Δ378-EGFP	GACGGC**AAGCTT**ATGGCGGGCTGCTGCTCCGTGCTCGGGTCC	TCA**GTCGAC**GTCTTCCACATACTTATATTTCTTGTCCCG
P2X4-AAA-EGFP	GACGGC**AAGCTT**ATGGCGGGCTGCTGCTCCGTGCTCGGGTCC	TACC**GTCGAC**CTGGTTCATCTCCCCCGAAGCAGCCTGCTCGGCGT
P2X4-AAA	GACGGC**AAGCTT**ATGGCGGGCTGCTGCTCCGTGCTCGGGTCC	TCA**CTCGAG**TCACTGGTTCATCTCCCCCGAAGCAGCCTGCTC

the Ca^{2+} sensitive dye Fura-2AM (2 μM, TEFLABS, Austin, TX) by incubation for 15 min at room temperature (RT). Subsequently, cells were removed from the Fura-2AM containing solution, and resuspended in a physiological saline solution used for imaging experiments that contained (in mM): 137 NaCl, 0.56 $MgCl_2$, 4.7 KCl, 1 Na_2HPO_4, 10 HEPES, 5.5 glucose, 1.26 $CaCl_2$, pH 7.4. Fura-2 loaded cells were allowed to adhere to a 25 mm glass coverslip for one minute before cells were locally superfused at a rate of at least 1 mL/min using a 0.5 mm diameter fused silica tube placed within 100 μm of the cells to be recorded. Rapid solution changes were accomplished utilizing an solenoid controlled perfusion system and gravity fed reservoirs (Warner Instruments, Hamden, CT). Imaging was performed using an inverted epifluorescence Nikon microscope with a 40× oil immersion objective lens (numerical aperture, 1.3). Fura-2 loaded cells were excited alternately with light at 340 and 380 nm using a monochrometer-based illumination system, and the emission at 510 nm was captured using a high speed, digital CCD camera (TILL Photonics, Pleasanton, CA). The fluorescence ratio of 340 nm/380 nm

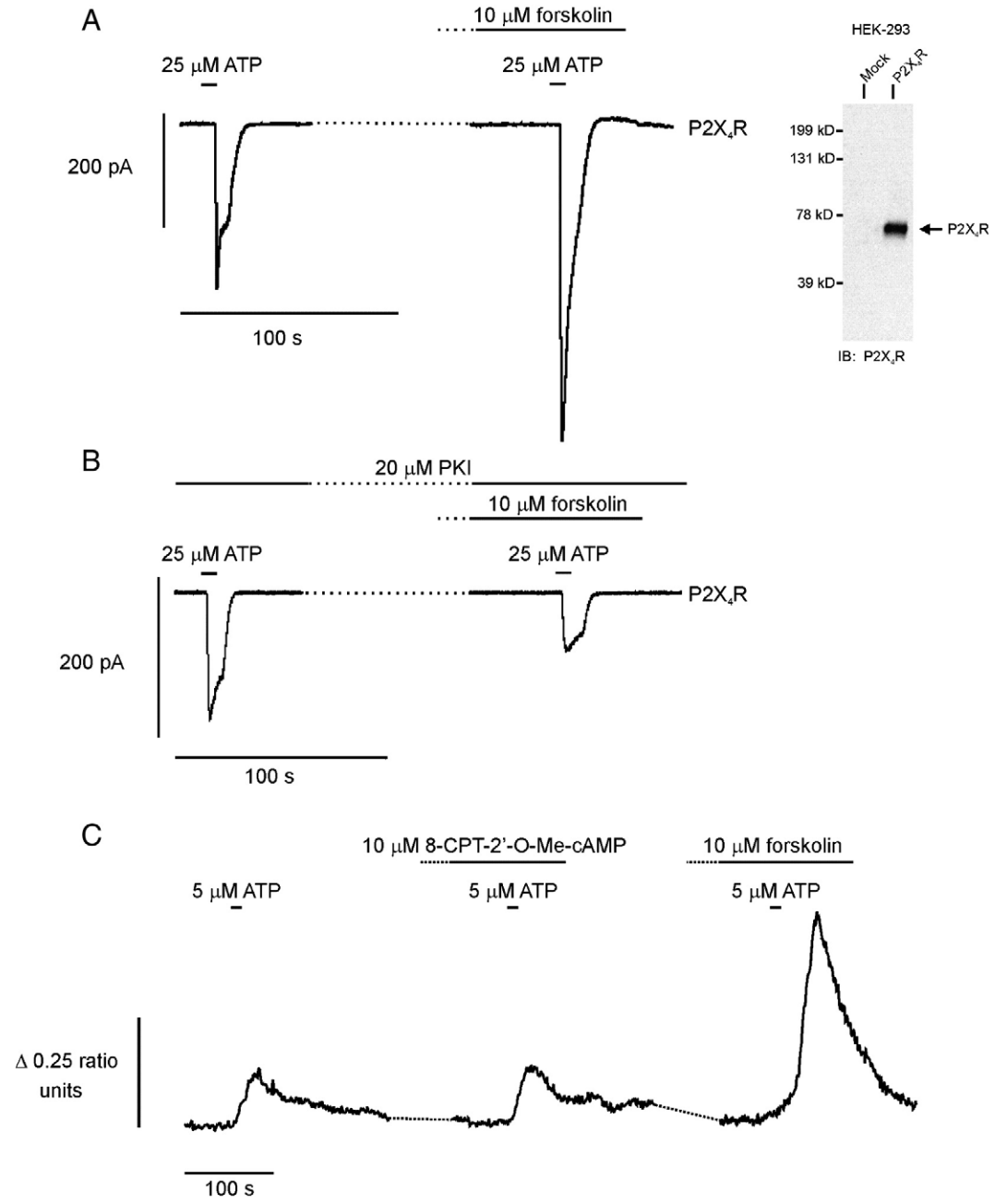

Fig. 1. The forskolin-mediated enhancement of $P2X_4R$ signaling is blocked by PKA inhibition. An immunoblot of mock-transfected HEK-293 cells shows that they lack $P2X_4R$, whereas $P2X_4R$ protein can readily be detected after transient overexpression of the receptor (inset). Transfected HEK-293 cells were whole cell patch clamped at a holding potential of −30 mV. (A) Treatment of $P2X_4R$-transfected HEK-293 cells with 25 μM ATP resulted in an inward current, which was enhanced by forskolin, consistent with our previous findings [19]. (B) Pretreatment with PKI, a cell-permeable PKA inhibitor, abolished the enhanced inward current following forskolin treatment in $P2X_4R$-transfected HEK-293 cells. The PKI/forskolin-treated second current was not significantly different in magnitude to previously published control values ($P2X_4R$ control, 76 ± 10% of initial response [19] *versus* $P2X_4R$ PKI/forskolin treatment, 66 ± 16%, $n = 8$ and $n = 4$ respectively, $p = 0.59$). However, there was a significant difference between the magnitude of the second response between PKI/forskolin and previously published forskolin-treated values ($P2X_4R$ forskolin treatment, 451 ± 101% of initial response [19] *versus* $P2X_4R$ PKI/forskolin treatment, 66 ± 16%, $n = 9$ and $n = 4$ respectively, $p = 0.017$ respectively). (C) $[Ca^{2+}]_i$ signals mediated by ATP in DT-40 3KO cells stably expressing $P2X_4R$ were not modulated by the EPAC specific analog 8-CPT-2′-O-Me-cAMP. In the same cells, forskolin treatment resulted in a significant potentiation of Ca^{2+} signals. The data are presented as the mean ± S.E. Each trace is representative of three or more experiments.

was calculated and all data is presented as the change in ratio units. Images were acquired at a rate of 1 Hz with an exposure of 20 ms. All imaging experiments were performed at RT, essentially as previously described [19,28]. Traces are from a single cell, representative of multiple individual cells in a particular experimental run, and *n* represents the number of experimental runs, with at least 3 cells per experimental run.

2.6. Whole cell patch clamp recordings

HEK-293 cells do not endogenously express P2X receptors. ATP-activated cation currents in transfected cells were recorded at a sampling rate of 1 kHz using an Axopatch 200A patch clamp amplifier (Axon Instruments, Union City, CA), Axon digital interface, and pCLAMP version 9.0 software under whole cell patch clamp conditions. To measure ATP-activated currents in HEK-293 cells, cells were perfused with an extracellular solution containing (mM): 140 NaCl, 5 CsCl, 1.2 $MgCl_2$, 1 $CaCl_2$, 10 HEPES, 10 D-glucose, pH 7.4. Internal patch solution contained (mM): 140 Cs-acetate, 1.22 $MgCl_2$, 10 HEPES-CsOH, 0.1 EGTA, 10 NaCl, 0.0365 $CaCl_2$, pH 7.2. Intervals of 2–3 min were allowed between patch rupture and stimuli to allow for equilibration with the patch pipette solution. HEK-293 cells were held at a holding potential of −30 mV. Experiments were performed at room temperature.

2.7. Total internal reflectance microscopy

TIRF microscopy was performed essentially as previously described [29]. Excitation light was provided by a 20 mW Argon Krypton laser (Omnichrome 43 series Meles Griot, Carlsbad, CA). The laser was directed through a light guide into a Till Photonics Polytrope TIRF condenser attached to the rear port of the microscope and through appropriate filters to select individual laser lines to a TIRF optimized high NA oil immersion objective (Olympus, Plan APO ×60, 1.45 NA) $P2X_4$-EGFP was excited using the 488 nm line of the laser isolated using a 488 nm band pass filter (BP 10 nm), 500 nm dichroic beam

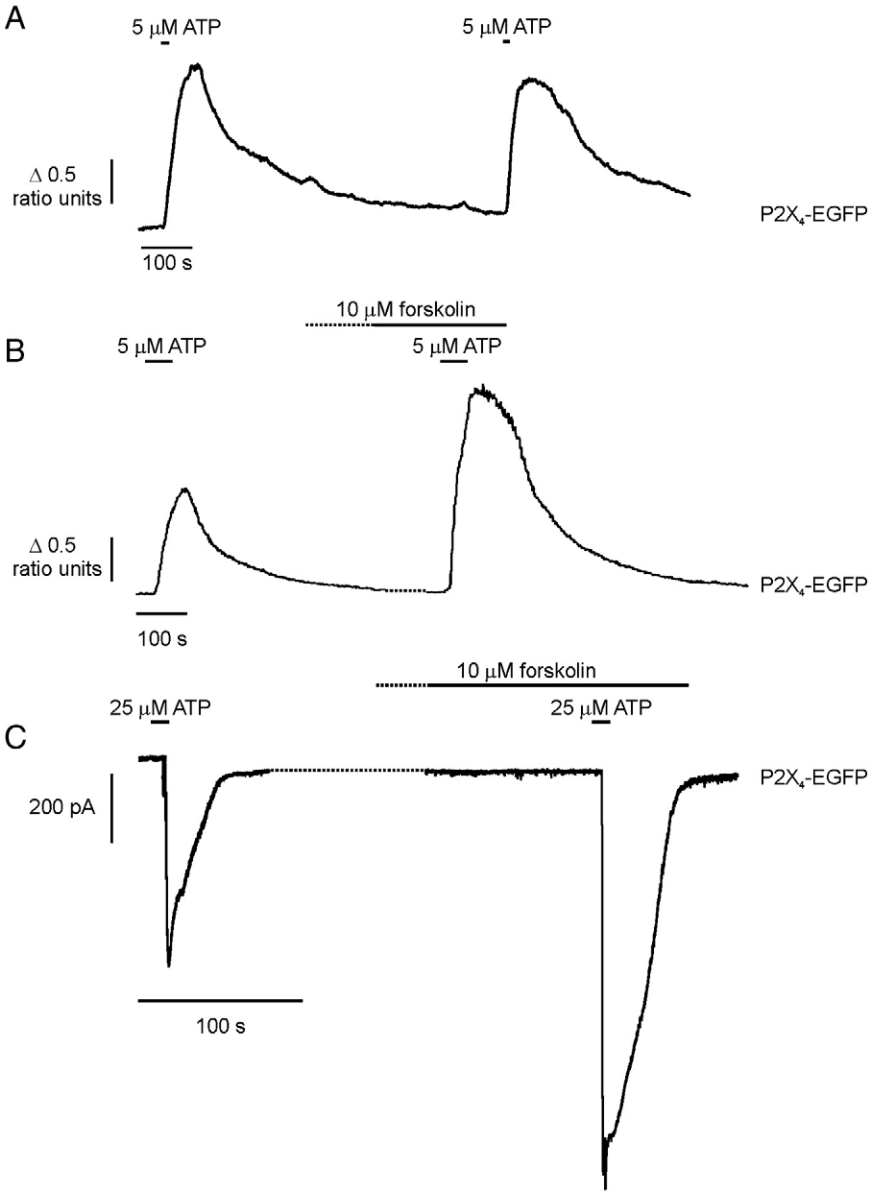

Fig. 2. cAMP-mediated potentiation of ATP-mediated Ca^{2+} signals in DT-40 3KO cells and ATP-activated currents in HEK-293 cells is retained in cells overexpressing $P2X_4$-EGFP. $P2X_4$-EGFP was generated by tagging the C-terminus of $P2X_4R$ with EGFP. (A) Multiple responses to ATP. (B) Forskolin treatment enhanced ATP-mediated Ca^{2+} signaling in DT-40 3KO cells transiently overexpressing $P2X_4$-EGFP receptors. (C) Forskolin enhanced ATP-activated current in HEK-293 cells overexpressing $P2X_4$-EGFP receptors. Traces are representative of 4 or more experiments.

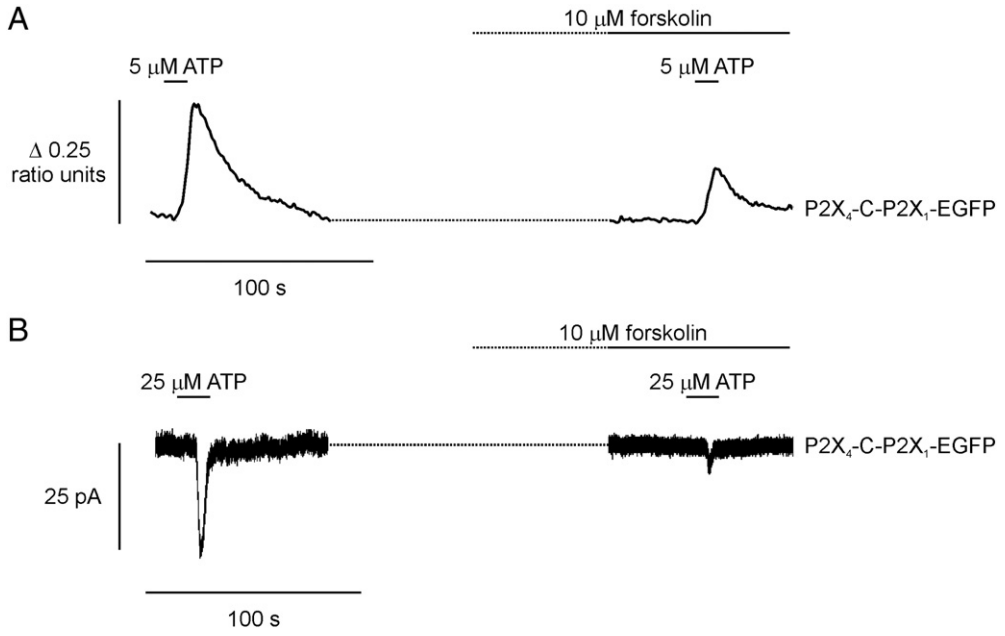

Fig. 3. A chimeric $P2X_4R$ with a $P2X_1R$ C-terminus is not enhanced by raising cAMP. $P2X_4$-C-$P2X_1$-EGFP was generated using the N-terminal, first transmembrane domain, and extracellular regions from $P2X_4R$ and replacing the second transmembrane domain and C-terminus with the corresponding amino acids from $P2X_1R$. (A) Transient transfection of $P2X_4$-C-$P2X_1$-EGFP receptors into DT-40 3KO cells elicited a Ca^{2+} spike when stimulated with ATP, which was no longer enhanced by forskolin treatment. (B) Forskolin did not enhance ATP-activated current in HEK-293 cells overexpressing chimeric $P2X_4$-C-$P2X_1$-EGFP receptors. Traces are representative of 4 or more experiments.

splitter and emitted light was collected through a 524 nm (BP 50 nm) band pass filter optimized for TIRF microscopy (BrightLine® series, Semrock, Rochester, NY). Images were collected every 5–10 s using a Cooke Sensicam QE camera controlled by Till Vision imaging suite. The laser was set to 50% power and angle of the beam was controlled within the objective lens by means of a computer controlled galvanometer driven mirror within the Polytrope. This TIRF angle was established (and remained fixed during the course of the studies) by imaging 200 nm polystyrene beads coated with fluorescent dye; TIR was judged to be occurring when discrete fluorescence of stationary, adhered beads ("landmark" beads) plus the occasional random "flashes" of beads transiently settling on the cover-glass were observed. TIRF microscopy was performed at 37 °C in a closed environmental chamber (Precision Plastics Inc., Beltsville MD) on the stage of an IX71 inverted microscope (Olympus, Center Valley, PA.).

2.8. Statistical analysis

Statistical significance was determined using unpaired *t* tests. Data from several cells in a particular experimental run were averaged, and experimental averages were used to calculate the mean ± S.E. Two-tailed *p* values of less than 0.05 were considered statistically significant.

3. Results

3.1. cAMP-induced enhancement of $P2X_4$ receptor signaling is blocked by PKA inhibition

A previous study from our laboratory has demonstrated that raising cAMP results in markedly augmented ATP-activated $P2X_4R$ signaling. The detailed molecular mechanism underlying this phenomenon was, however, not established [19]. An obvious posit to account for the potentiation is that raising cAMP activates PKA and either phosphorylates the $P2X_4R$ directly or alternatively an accessory protein. To directly test if PKA activation is required for this potentiation, we investigated if inhibition of PKA could abrogate the enhanced signaling observed after raising cAMP [19]. Two systems were chosen to serve as expression platforms to evaluate $P2X_4R$ function in isolation: DT-40 chicken pre-B lymphocytes and HEK 293 cells. The former do not express any purinergic receptors, while the latter are null for P2XR. Ca^{2+} signaling events were monitored in DT-40 3KO cells and the channel activity was measured directly using

Table 2
Summary of mutant $P2X_4$ receptors and cAMP-dependent regulation. Note that the presence or absence of the endocytosis motif (highlighted in gray) corresponds with whether the construct is enhanced by raising cAMP (shown by +) or not (shown by −).

$P2X_4$-WT	N– NVGSGLALLGVATVLCDVIVLYCMKKKYYYRDKKYKYVEDYEQGLSGEMNQ (TM2; 338–378–388)	+
$P2X_4$-Δ384	N– NVGSGLALLGVATVLCDVIVLYCMKKKYYYRDKKYKYVEDYEQGLS (TM2; 338–378)	+
$P2X_4$-Δ378	N– NVGSGLALLGVATVLCDVIVLYCMKKKYYYRDKKYKYVED (TM2; 338–378)	−
$P2X_4$-AAA	N– NVGSGLALLGVATVLCDVIVLYCMKKKYYYRDKKYKYVEDAEQAASGEMNQ (TM2; 338–378–388)	−

whole cell patch clamp techniques in HEK-293 cells following transfection [19,22]. An immunoblot, Fig. 1 *inset*, confirmed the lack of $P2X_4R$ in mock-transfected HEK-293 cells, whereas $P2X_4R$-transfected HEK-293 cells displayed a single distinct band. Treatment with forskolin significantly enhanced the ATP-induced inward current in $P2X_4R$-expressing HEK-293 cells (Fig. 1A), in agreement with our previously published findings [19]. Incubation with myristolylated $PKI_{6–22}$, a specific, cell-permeable PKA inhibitor [30], abolished this potentiation (Fig. 1B). The second response after PKI and forskolin treatment was $66 \pm 16\%$ with respect to the initial stimulation ($n = 5$). This was not significantly different from previously published control responses without forskolin [19]. These data clearly demonstrate that PKA activation is required for the observed effect. In further support of this contention, H89, a non-selective serine/threonine protein kinase inhibitor also abrogated the effect of PKA activation (data not shown).

EPAC proteins represent an additional family of PKA-independent cAMP effectors. Several lines of evidence make it unlikely that these proteins regulate $P2X_4R$ signaling. First, regulation through EPAC proteins is unaffected by PKA inhibition (29) and secondly, the EPAC selective activator 8-CPT-2′-O-Me-cAMP was unable to reproduce the potentiation of Ca^{2+} signaling observed following PKA activation in DT-40 cells stably expressing the $P2X_4R$ (Fig. 1C).

3.2. Defining the region of the $P2X_4R$ required for PKA-dependent enhancement

Next, a mutational strategy was employed to identify the specific region of the $P2X_4R$ that was required for PKA-mediated potentiation. This approach was undertaken to reveal potential PKA phosphorylation sites, implicate potential binding partners, and provide key insight into the mechanism of the potentiation. Wild-type and mutant receptors were tagged at the C-terminus with EGFP to facilitate identification of expressing cells and to validate the PM localization of mutated receptors. The $P2X_4R$-EGFP was functional, since multiple exposures to ATP resulted in repetitive elevations in $[Ca^{2+}]_i$ similar to wild-type (Fig. 2A, 2nd response $85 \pm 7\%$ of initial response, $n = 5$). In addition, forskolin treatment augmented the 2nd ATP-evoked Ca^{2+} signal in DT-40 3KO cells expressing $P2X_4R$-EGFP (Fig. 2B, $232 \pm 43\%$ over the initial control response in the presence forskolin, $n = 5$). Furthermore, forskolin treatment increased ATP-evoked inward currents in HEK-293 cells expressing $P2X_4R$-EGFP (Fig. 2C, $156 \pm 23\%$ over the initial control response, $n = 4$). These results are summarized in Fig. 7A–B.

Both the N- and C-termini of $P2X_4R$ face the cytoplasm and thus are potentially subject to modulation by cellular factors. Of particular note, sequence analysis does not reveal any recognizable PKA consensus phosphorylation sites based on the canonical RRXS/T or RXXS/T motifs in either of these regions. The N-termini of P2XR are fairly short (≤30 amino acids, 27 amino acids in $P2X_4R$), and the C-termini diverge in sequence and length considerably [2]. In addition, $P2X_4R$ and $P2X_7R$ have high sequence similarity in the N-terminal region, but $P2X_7R$ signaling is not affected by raising cAMP levels [19]. In total, this information indicates that the $P2X_4R$ N-terminus may not be a promising candidate region subject to this regulation [18]. Thus, initial mutational analysis was performed in the C-terminus. A chimera in which the C-terminus of the $P2X_4R$ was substituted with the C-terminus of the $P2X_1R$ (P2X4-C-P2X1-EGFP) was generated. The

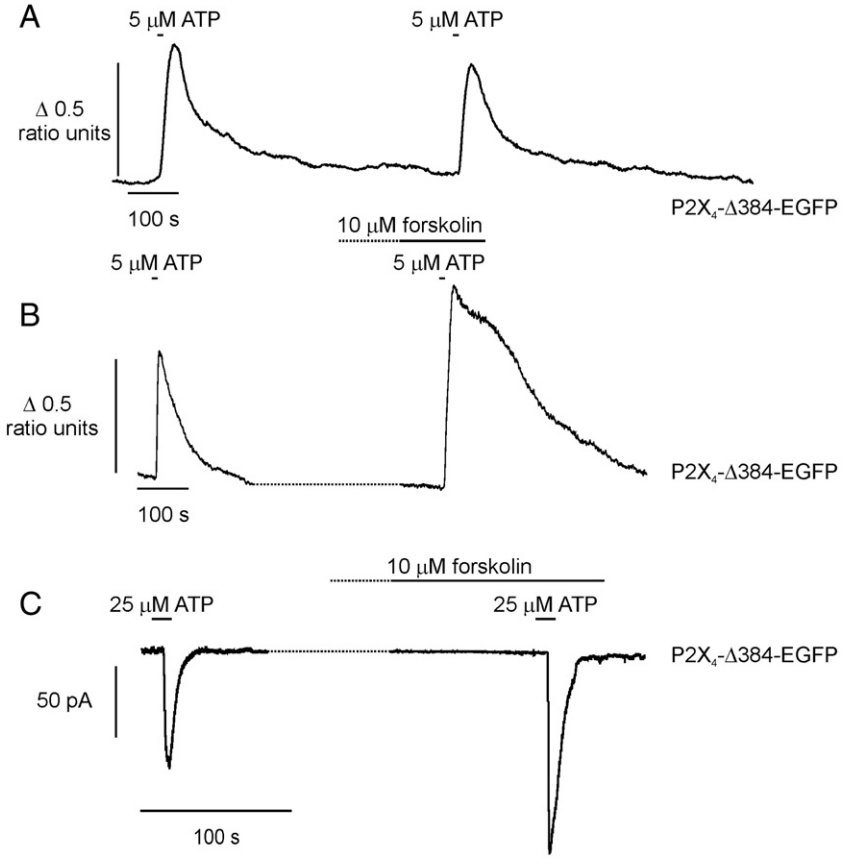

Fig. 4. cAMP-mediated potentiation of ATP-mediated Ca^{2+} signals in DT-40 3KO cells and ATP-activated currents in HEK-293 cells is retained in cells overexpressing the truncation mutant receptor $P2X_4$-Δ384-EGFP. $P2X_4$-Δ384-EGFP was generated by removing the last 5 amino acids of the $P2X_4R$ C-terminus. (A) Multiple responses to ATP exposure in cells expressing this construct. (B) Forskolin treatment enhanced ATP-mediated Ca^{2+} signaling in DT-40 3KO cells overexpressing $P2X_4$-Δ384-EGFP receptors. (C) Forskolin potentiated ATP-activated currents in HEK-293 cells overexpressing $P2X_4$-Δ384-EGFP receptors. Traces are representative of 4 experiments.

rationale for generation of this construct was two-fold: first, $P2X_1R$ forms a hetero-channel with $P2X_4R$ subunits and thus would likely yield a functional channel and secondly, because $P2X_1R$ signaling is unaffected by PKA activation this chimera might reveal structural/sequence requirements for the effect of PKA [2,13]. $P2X_4$-C-$P2X_1R$-EGFP were expressed in either DT-40 3KO cells or HEK-293 cells and similar experimental paradigms were used to those shown in Fig. 2. Stimulation with ATP resulted in a Ca^{2+} transient or inward cation current similar to cells expressing the $P2X_4$-EGFP receptor. However, treatment with forskolin did not enhance the ATP-mediated Ca^{2+} signals (Fig. 3A) or inward currents (Fig. 3B). The kinetics of the currents in the chimera were different from the wild-type receptor, but superficially resembled the rapid desensitization kinetics of the $P2X_1R$ [2]. These data suggest that PKA regulation of $P2X_4R$ is dependent on determinants present in the C-terminus of $P2X_4R$, which are absent in the C-terminus of $P2X_1R$.

3.3. $P2X_4R$ truncations reveal an important region in the C-terminus required for PKA-mediated regulation

To further define the regions important for PKA regulation in the C-terminus, two $P2X_4R$ C-terminal truncations were generated (see Table 2). The effect of PKA activation was retained in a construct designated $P2X_4$-Δ384-EGFP where the terminal 5 amino acids were removed from the receptor (Fig. 4A–C). In DT-40 3KO cells the 2nd Ca^{2+} response in the absence of forskolin was $60 \pm 4\%$ ($n = 11$) of the initial challenge (Fig. 4A), while treatment with forskolin significantly enhanced the Ca^{2+} signal (Fig. 4B, $311 \pm 55\%$ over the initial control response, $n = 4$). Furthermore, the ATP-induced inward current in HEK-293 cells expressing $P2X_4$-Δ384-EGFP was also increased following exposure to forskolin (Fig. 4C, $158 \pm 42\%$ over the initial control response, $n = 4$). In comparison, the 2nd ATP-evoked current in HEK-293 cells in the absence of forskolin was $77 \pm 12\%$ ($n = 3$) of the initial response. The effect of PKA observed in this construct was not significantly different from that observed in cells expressing the wild-type $P2X_4R$-EGFP (see data summary Fig. 7A–B, $p = 0.29$ and $p = 0.97$ respectively).

A more extensive truncation, where a total of 11 amino acids were removed from the receptor designated $P2X_4$-Δ378-EGFP, was however not regulated following PKA activation. As shown in Fig. 5A–C, PKA activation did not increase either Ca^{2+} signals in DT-40 3KO cells (Fig. 5A–B, $69 \pm 6\%$ ($n = 9$) over initial control in the absence of forskolin and $52 \pm 4\%$ ($n = 5$) following exposure to forskolin) or the inward current in HEK-293 cells (Fig. 5C, $64 \pm 8\%$ ($n = 3$) over initial control in the absence of forskolin and $55 \pm 13\%$ ($n = 6$) following exposure to forskolin). Of note, deletion of these additional amino acids removed a putative tyrosine based sorting motif (YEQGL), which has been implicated in $P2X_4R$ trafficking out of the PM [31,32].

It is known that $P2X_4R$ constitutively internalize and then recycle back to the surface PM [33]. This cycling was proposed to be a mechanism for rapidly regulating the functional expression of receptors. Agonist application (100 μM ATP for 15 min) has been shown to increase the internalized fraction of $P2X_4R$ by approximately 60%, consistent with findings published on $P2X_1R$ [33,34]. The YXXGL motif has been reported to be required for receptor internalization and recognition by the adapter protein 2 (AP2) complex and disruption of this motif results in decreased internalization and enhanced surface expression [31].

3.4. PKA regulation of $P2X_4R$ requires an intact YXXGL motif in the C-terminus

To determine if this motif was important for regulation of $P2X_4R$ by PKA, a full length receptor mutant was generated with only the YXXGL

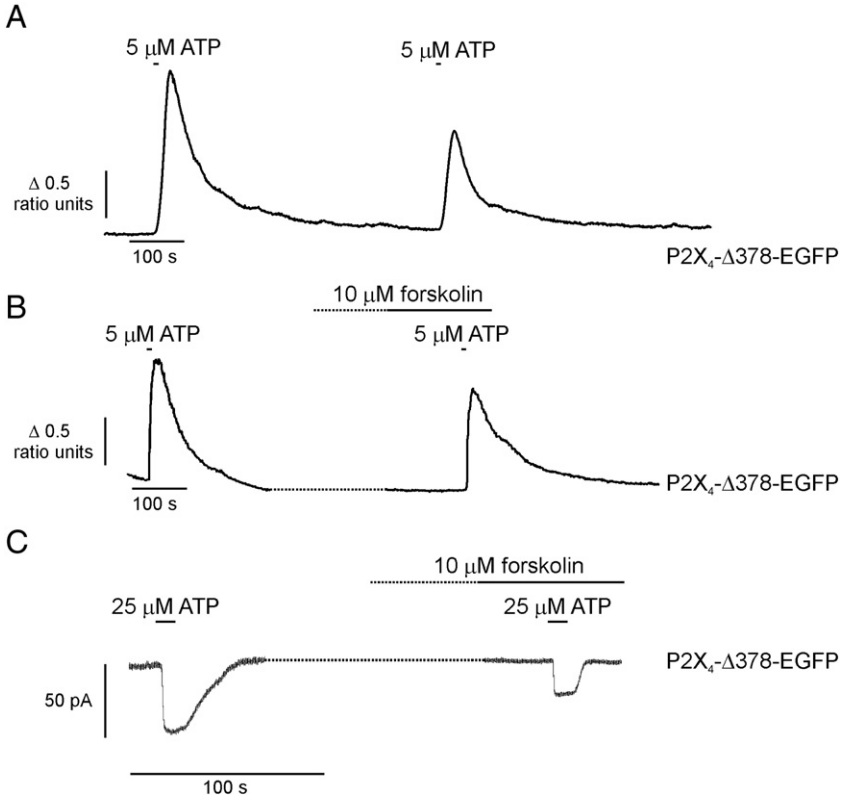

Fig. 5. Truncation of 11 amino acids in the $P2X_4R$ C-terminus prevents cAMP-mediated potentiation of ATP-mediated signaling. $P2X_4$-Δ378-EGFP was generated by removing the last 11 amino acids of the $P2X_4R$ C-terminus. (A) Multiple responses to ATP exposure in cells expressing this construct. (B) Forskolin treatment did not enhance ATP-mediated Ca^{2+} signaling in DT-40 3KO cells overexpressing $P2X_4$-Δ378-EGFP receptors. (C) Forskolin did not augment ATP-activated currents in HEK-293 cells overexpressing $P2X_4$-Δ378-EGFP receptors. Traces are representative of 5 or more experiments.

motif disrupted. Three alanine substitutions were made in this receptor to yield AXXAA at amino acids 378–382. The effect of PKA regulation on this mutant was not present in DT-40 3KO cells (57 ± 5% of the initial response in the absence (Fig. 6A, $n = 6$) or 43 ± 12% over the initial response in the presence of forskolin (Fig. 6B, $n = 7$)) Similarly, the effect of PKA activation was eliminated in HEK-293 cells expressing this construct (46 ± 10% over the initial control response, Fig. 6C, ($n = 9$)). These data are similar to those obtained in cells expressing the $P2X_4$-Δ378-EGFP construct shown in Fig. 5A–C, which also had this motif disrupted (see data summary Fig. 7A–B, $p = 0.56$ and $p = 0.59$ respectively). An amino acid alignment of the C-terminus of the mutants is shown in Table 2, which demonstrates the absolute requirement for the YXXGL endocytosis motif to be intact for cAMP-mediated enhancement to occur (highlighted in gray).

Importantly, this mutational analysis also argues against direct $P2X_4R$ phosphorylation by PKA, since as previously noted there are no PKA consensus sites in regions required for the functional effect. In fact, there is only one serine residue present in the entire intracellular C-terminal region at position 383 (not a PKA consensus site (QGL***S***)). In support of this mutational and sequence analysis, extensive efforts to detect direct $P2X_4R$ phosphorylation by PKA were unsuccessful. For example, both *in vivo* and *in vitro* attempts to demonstrate phosphorylation of $P2X_4R$ failed under conditions were phosphorylation of known PKA substrates could be clearly shown (Supplemental Fig. 1). These data strongly suggest that, while PKA activation is absolutely required, the potentiation of $P2X_4R$ signaling does not involve direct phosphorylation of the receptor. In addition, mutational analysis suggests that the target of PKA is a protein which interacts with the putative tyrosine based sorting motif.

3.5. PKA activation results in accumulation of $P2X_4$-EGFP near the plasma membrane

A HEK-293 cell line was created which stably expressed $P2X_4$-EGFP. We next performed TIRF microscopy to monitor the movement of tagged receptors in the vicinity of the PM. The evanescent field established following TIR allows the excitation of fluorophores within 125–175 nm of the PM. Following establishment of TIR, the fluorescence of $P2X_4$-EGFP was manifested as discrete fluorescent puncta (contrast wide-field image and TIRF image in Fig. 8A). Under resting conditions, a significant proportion of these puncta were mobile and moved apparently randomly in and out of the evanescent field. Following forskolin treatment, the puncta appeared to coalesce and be retained for extended periods of time in larger areas as shown in representative images (Fig. 8B) and kinetic line plots (Fig. 8C) for 3 areas indicated in the gray scale image (Fig. 8B). This accumulation of fluorescence did not occur as a function of morphological changes in HEK cells initiated by PKA because a membrane targeted YFP (myr-YFP) did not similarly accumulate in large puncta following PKA activation (data not shown). Further experiments were performed in which TIRF fluorescence was monitored in cells transiently expressing $P2X_4$-AAA-EGFP (Fig. 8D). In contrast to $P2X_4$-EGFP expressing cells, no increase in near-PM fluorescence was observed in these cells following forskolin exposure. These data indicate that $P2X_4R$ are

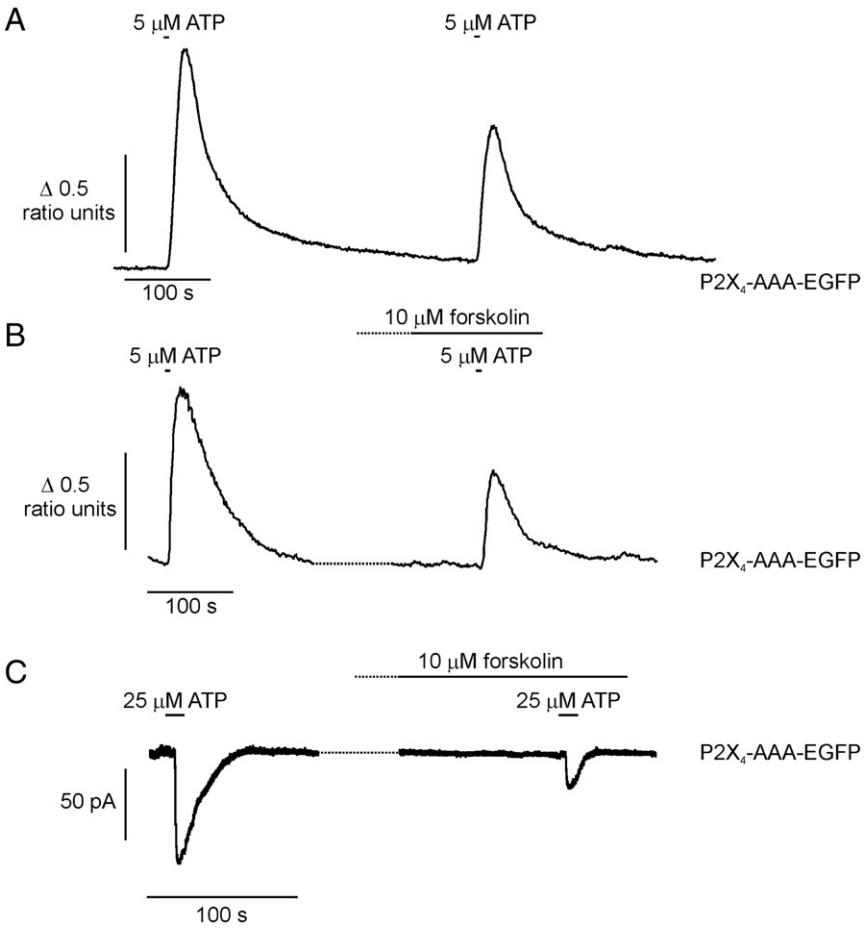

Fig. 6. Disruption of the YXXGL endocytosis motif in the full length $P2X_4R$ also prevents cAMP-mediated potentiation of ATP-mediated signaling. $P2X_4$-AAA-EGFP was generated by three alanine point mutations in the YXXGL motif of the full length $P2X_4R$. (A) Multiple responses to ATP exposure in cells expressing this construct. (B) Forskolin treatment did not enhance ATP-mediated Ca^{2+} signaling in DT-40 3KO cells overexpressing $P2X_4$-AAA-EGFP receptors. (C) Forskolin did not enhance ATP-activated currents in HEK-293 cells overexpressing $P2X_4$-AAA-EGFP receptors. Traces are representative of 6 or more experiments.

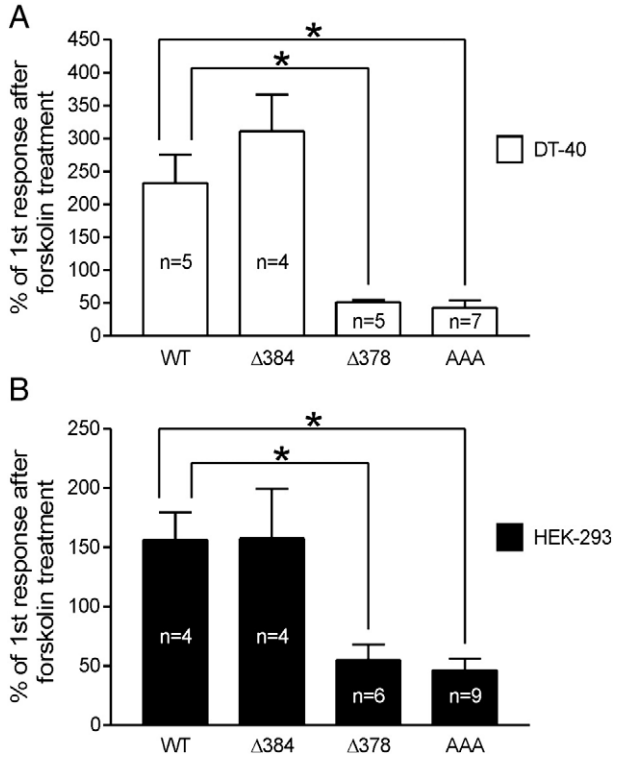

Fig. 7. Data summary of ATP-mediated Ca^{2+} signals in DT-40 3KO cells and ATP-activated currents in HEK-293 cells overexpressing $P2X_4R$ mutants. (A) Data summary of ATP-mediated Ca^{2+} signaling in DT-40 3KO cells from paired experiments, where the forskolin-treated second response is expressed as a percentage of the control-treated first response (white bar graph). (B) Data summary of ATP-activated currents in HEK-293 cells from paired experiments, where the forskolin-treated second response is expressed as a percentage of the control-treated first response (black bar graph). The data are presented as the mean ± S.E. (*, $p<0.05$).

retained close to the plasma membrane following PKA activation and this is consistent with the proposal that this may contribute to the augmentation of purinergic signaling following PKA treatment. Nevertheless, attempts to demonstrate biochemically that $P2X_4R$ accumulated at the PM following forskolin treatment using a biotinylation paradigm were unsuccessful. The reason for this is unclear, but may reflect the difficulties in detecting changes by this technique of only a subpopulation of a protein which is itself expressed in relatively low abundance.

3.6. Dominant-negative dynamin K44A blocks forskolin-mediated potentiation of $P2X_4R$ signaling

A complimentary approach was utilized to determine if the forskolin-induced enhancement of $P2X_4R$ signaling involves endocytosis through the sorting motif. In addition to mutating the endocytosis motif on the $P2X_4R$, the requirement for the interaction of the $P2X_4R$ with the endocytosis machinery *per se* was tested. Experiments were performed using a dominant-negative mutant dynamin construct (dynamin K44A), which is not capable of clatherin/AP2 mediated endocytosis [35]. DT-40 3KO cells stably expressing wild-type $P2X_4R$ were utilized to maintain similar $P2X_4R$ expression levels between different experiments. Stable $P2X_4R$ expressing cells were then either co-transfected with empty vector (Mock) and HcRed (for positive identification of transfected cells) or dynamin K44A and HcRed. There was a trend for dynamin K44A transfected cells to exhibit an increased ATP-mediated Ca^{2+} response, however the Ca^{2+} responses were not statistically different from mock-transfected cells (Mock; 0.13 ± 0.05 ratio units over baseline *versus* K44A; 0.33 ± 0.13, $n=17$ and $n=11$ respectively, $p=0.14$), suggesting dynamin K44A enhanced $P2X_4R$ surface expression. These findings are consistent with experiments that demonstrated enhanced ATP-mediated $P2X_4R$ current amplitudes when using either dominant-negative μ2 (also called AP-50) subunits from the AP2 complex or dominant-negative Esp15, which interacts with the AP2 complex [36]. Dominant-negative μ2 subunits have also been reported to increase $P2X_4R$ surface expression [31]. Mock-transfected DT-40 3KO cells stably expressing $P2X_4R$ still exhibited significantly augmented ATP-mediated Ca^{2+} signals following forskolin treatment (Fig. 9A + C, Mock control treatment; 96 ± 6% of 1st response *versus* Mock forskolin treatment; 190 ± 23% of 1st response, $n=4$ and $n=13$ respectively, $p=0.04$). However, expression of dominant-negative dynamin K44A in DT-40 3KO cells stably expressing $P2X_4R$ resulted in ATP-mediated Ca^{2+} signals that were not augmented following forskolin treatment (Fig. 9B). This result was significantly different from mock-transfected cells (Fig. 9C, Mock forskolin treatment; 190 ± 23% of 1st response *versus* K44A forskolin treatment; 114 ± 18% of 1st response, $n=13$ and $n=8$ respectively, $p=0.03$). In fact, forskolin treatment had no significant effect over control treatment when dynamin K44A was expressed (Fig. 9C, K44A control treatment; 97 ± 20% of 1st response *versus* K44A forskolin treatment; 114 ± 18% of 1st response, $n=3$ and $n=8$ respectively, $p=0.61$).

TIRF experiments were next performed to corroborate the above data that expression of dominant-negative K44A dynamin eliminated the effects of forskolin treatment by disrupting trafficking to/from the PM. HEK-293 cells stably expressing $P2X_4R$-EGFP were transiently transfected with cDNA encoding K44A dynamin and HcRed to positively identify transfected cells. Fig. 10 illustrates a representative experiment typical of 6 others from 3 transfections. Fig. 10A shows a bright field image of a group of cells (Fig. 10Ai), a number of which express HcRed and thus presumably K44A dynamin (Fig. 10Aii). As measured by HcRed fluorescence a range of expression was noted, but ~70% of cells expressed detectable fluorescence. $P2X_4R$-EGFP fluorescence observed by conventional fluorescence microscopy was clearly visualized in the PM as well as in intracellular compartments (Fig. 10Aiii). Under TIRF conditions, as shown previously, isolated fluorescent puncta were evident, representing points of close apposition of the PM to the coverslip (Fig. 10Aiv). In cells expressing prominent HcRed fluorescence (>500 gray levels) the intensity of $P2X_4R$-EGFP TIRF fluorescence often appeared brighter than in neighboring cells with less HcRed fluorescence (arrow in Fig. 10Aii and 10Aiv). In contrast to control conditions (Fig. 8), the puncta observed in these experiments appeared relatively immobile as can be seen in representative images captured over many minutes (Fig. 10Ba–e) Importantly, the distribution and size/intensity of the puncta was unaltered by forskolin treatment (Fig. 10B–C). These data are consistent with expression of dominant-negative dynamin leading to accumulation of $P2X_4R$-EGFP in the plasma membrane as a result of attenuated endocytosis and further that inhibition of the trafficking machinery effectively eliminates the effects of forskolin to increase the amount of $P2X_4R$ close to the PM. In summary, mutation of the $P2X_4R$ sorting motif or disruption of the endocytosis machinery is sufficient to prevent PKA-mediated potentiation of $P2X_4R$ signaling and thus strongly suggests that the underlying mechanism involves modulation of endocytotic machinery.

4. Discussion

This study reports that PKA-mediated regulation of $P2X_4R$ signaling requires the internalization motif YXXGL. A likely explanation is that raising cAMP can inhibit constitutive endocytosis resulting in an increase in the number of functional $P2X_4R$ at the PM. Because the YXXGL motif on $P2X_4R$ can interact with the μ2 subunit of the AP2 complex, possible targets for PKA may include proteins in this

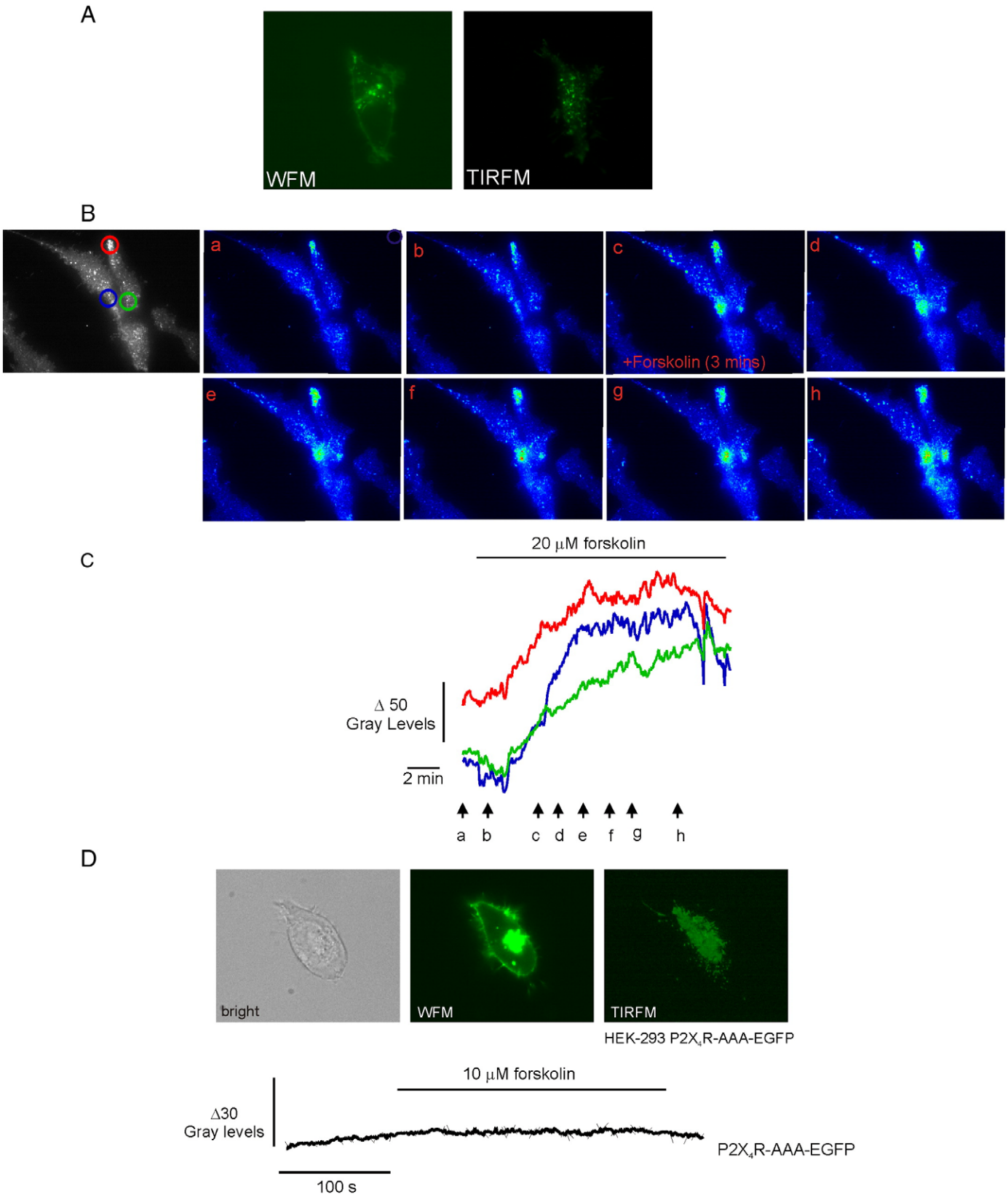

Fig. 8. PKA activation increases the number of $P2X_4$-EGFP in the vicinity of the plasma membrane. Experiments were performed monitoring the movement of $P2X_4$-EGFP using TIRF microscopy in cells stably expressing the receptor. (A) Shows the fluorescence of $P2X_4$-EGFP in wide field (WFM) and following establishing TIRF mode (TIRFM). (B) Shows a series of images obtained at the time-points indicated in (C) for a group of HEK-293 cells stably expressing $P2X_4$-EGFP. (C) Shows kinetic plots from 3 regions of interest indicated in the gray scale image in (B). Following forskolin treatment fluorescence puncta grew larger and increased intensity. An exemplar experiment showing three regions of interest typical of data from 7 experimental runs. (D) Shows similar experiments in which $P2X_4$-AAA-EGFP was transiently expressed in cells. Forskolin treatment did not alter the distribution of this mutant receptor.

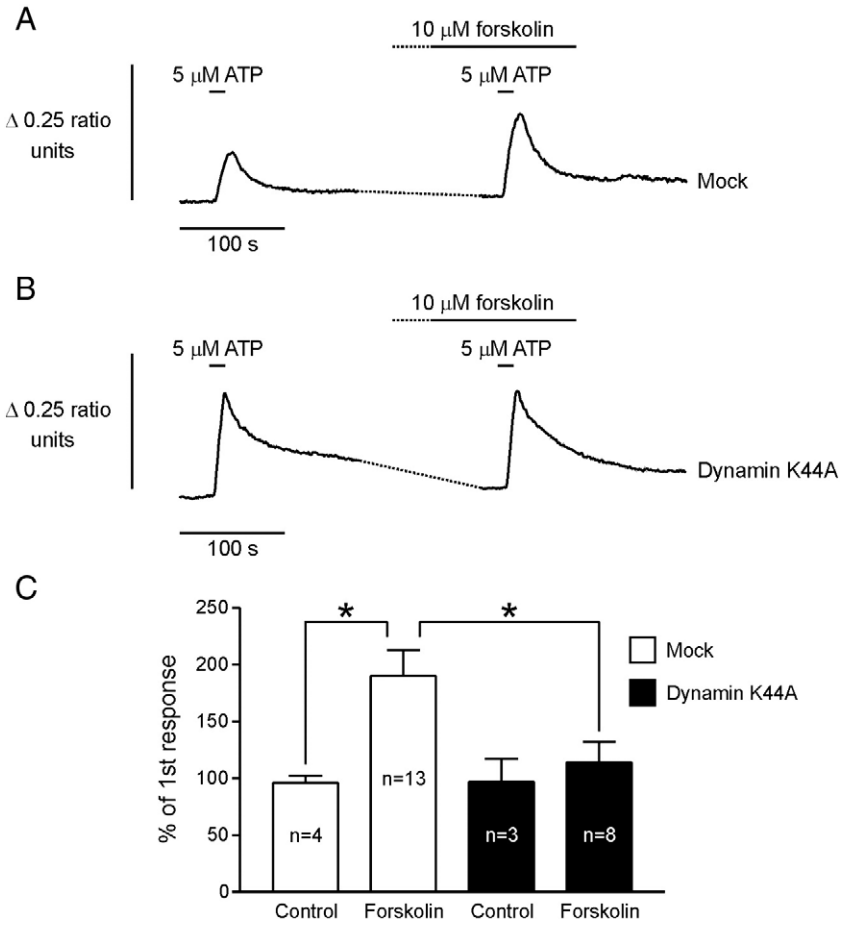

Fig. 9. DT-40 3KO cells stably expressing $P2X_4R$ exhibit forskolin-mediated enhancement of ATP-evoked Ca^{2+} signals, which can be blocked by dominant-negative dynamin K44A expression. (A) ATP-activated Ca^{2+} signals in mock-transfected DT-40 3KO cells stably expressing $P2X_4R$ are enhanced by forskolin treatment. (B) Forskolin treatment had no effect on ATP-mediated Ca^{2+} signals in DT-40 3KO cells stably expressing $P2X_4R$ and transiently overexpressing dominant-negative dynamin K44A. Traces are representative of eight or more experiments. (C) Data summary of ATP-mediated Ca^{2+} signaling in DT-40 3KO cells stably expressing $P2X_4R$ from paired experiments after transient mock- or dynamin K44A-transfection (white and black bar graph, respectively), where the control- or forskolin-treated second response is expressed as a percentage of the control-treated first response.

complex [32]. Of interest, the μ2 subunit has been shown to be phosphorylated on a threonine residue [37]. In addition to μ2, the AP2 complex also contains α and β2 subunits, both of which have been shown to be phosphorylated *in vivo* [38]. Future experiments are necessary to identify the protein(s) involved in this novel PKA potentiation mechanism of $P2X_4R$ signaling.

Data in the present study supports the notion that PKA activity increases the amount of functional $P2X_4R$ at the PM through an effect on the endocytosis machinery. However, the possibility of an effect on the receptor at the single channel level, resulting in an increase in the single channel conductance ($i_{(cation)}$) and/or the open probability (P_o), cannot be excluded. In support of this idea, ivermectin, in addition to causing an increase in surface expression of $P2X_4R$, has also been shown to modulate $P2X_4R$ single channel conductance and open probability [36,39].

The work presented in this study adds to a growing body of literature that suggests that protein kinase regulation of P2X receptors does not involve direct receptor phosphorylation. Vial et al. were the first to suggest that PKC-mediated modulation of $P2X_1R$ did not involve direct receptor phosphorylation [40]. We recently demonstrated that PKC-mediated modulation of $P2X_3R$ signaling does not result from direct receptor phosphorylation [22]. This study now presents evidence that PKA regulation of $P2X_4R$ is unlikely to involve direct receptor phosphorylation. In total, these data lend support to a common theme whereby protein kinase modulation of P2XR signaling involves accessory proteins. Further study is necessary to ascertain whether common central mechanisms are involved in phosphoregulation of P2XR in general.

The major finding of this study, that PKA activation can significantly enhance $P2X_4R$-mediated signaling could have broad physiological consequences in tissues with predominant expression of these receptors given that PKA activation is the end point of a ubiquitous signaling system. For example, in salivary acinar cells Ca^{2+} flux through $P2X_4R$ only generates a minimal cytosolic Ca^{2+} signal in absence of PKA activation [19]. Strikingly as cAMP is elevated, whole cell current through the channel and the resultant Ca^{2+} change are markedly increased [19]. These Ca^{2+} signals would be predicted to significantly increase both fluid and protein secretion from the gland under these conditions. Since parasympathetic and sympathetic co-stimulation of the gland is the usual physiological situation, this form of regulation in all probability should be considered the norm. Other examples where this mode of modulation may be significant include bronchiolar epithelium were $P2X_4R$ are abundant and play a key role in maintaining the beating of cilia required to move the mucus layer to clear airways [41]. Augmented Ca^{2+} entry following sympathetic input through $P2X_4R$ could conceivably be of therapeutic benefit in situations such as cystic fibrosis where mucus accumulates and is slowly cleared [41]. $P2X_4R-/-$ mice are hypertensive [42]. It is possible that phosphoregulation of $P2X_4R$ could also play a role in the regulation of blood pressure. For example, enhanced [Ca^{2+}] as a consequence of increased $P2X_4R$ activity in the endothelium of the vasculature could increase nitric oxide release, resulting in

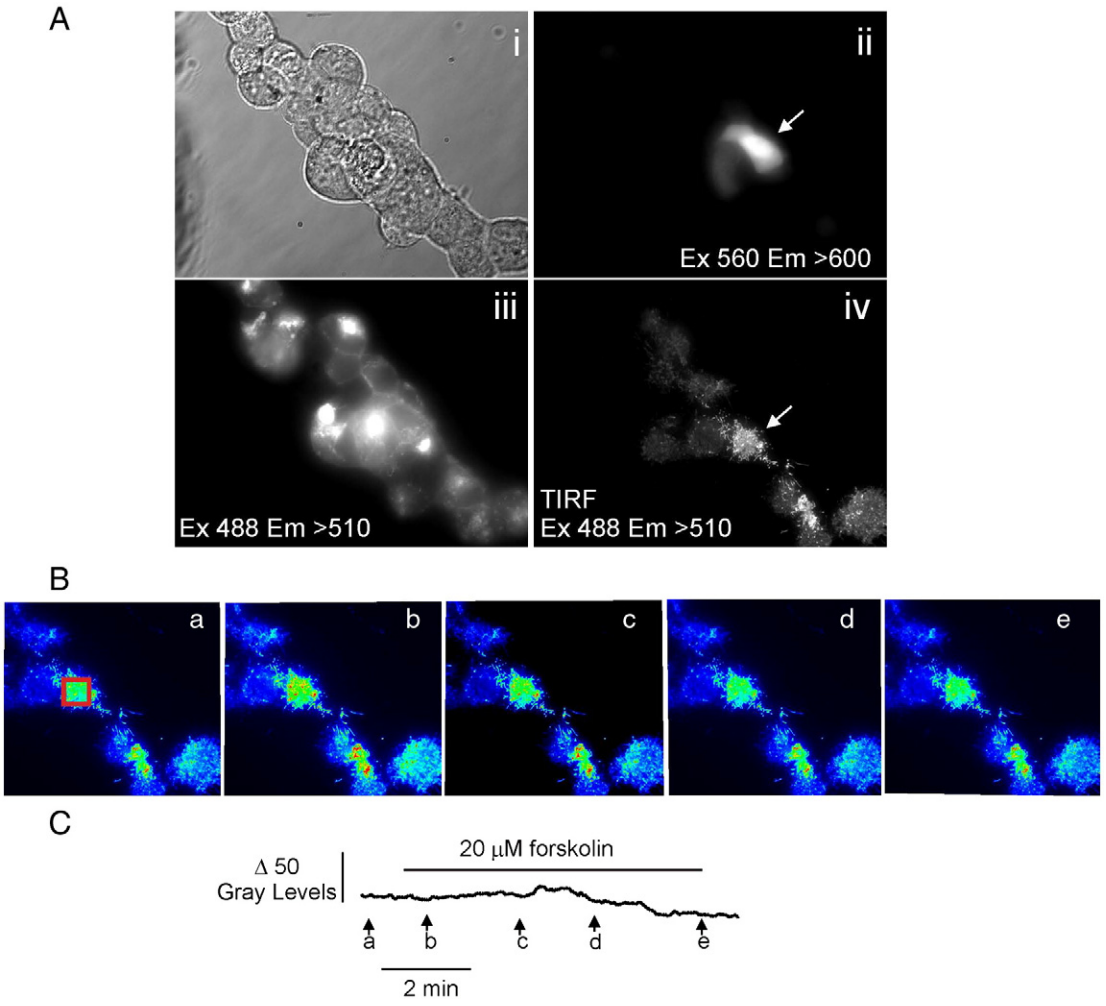

Fig. 10. Expression of dominant-negative K44A dynamin eliminates the forskolin-induced retention of $P2X_4$-EGFP close to the PM. (Ai) Bright field image of HEK-293 cells stably expressing $P2X_4$-EGFP and transiently co-expressing HcRed and K44A dynamin. (Aii) Wide-field fluorescence image indicating HcRed expression (Ex 560 nm; Em > 600 nm). (Aiii) Wide-field fluorescence image of $P2X_4$-EGFP (Ex 488 nm; Em 510 nm). (Aiv) TIRF fluorescence image of $P2X_4$-EGFP. (B) Series of TIRF images captured at the time-points indicated in C in which the cells were exposed to forskolin. (C) Kinetic line plot of average fluorescence from the red box shown in B.

vasodilatation [42]. Greater knowledge of $P2X_4R$ signaling could also help increase our understanding of neuropathic pain, as $P2X_4R$ are involved in deranged sensory transduction observed in tactile allodynia, a condition where intense pain is generated from light touches of the skin that were previously innocuous [42].

In summary, PKA-mediated modulation of the $P2X_4R$ requires an intact YXXGL endocytosis motif in the C-terminus. Mutational analysis of this region suggests that this regulation does not involve $P2X_4R$ phosphorylation. Instead, the mechanism of potentiation appears to involve regulation of the endocytosis pathway, since it can be blocked by disruption of either the endocytosis motif on the receptor or the endocytosis machinery. PKA-mediated inhibition of endocytosis could increase the number of $P2X_4R$ at the PM, hence increasing the effects of subsequent ATP stimulation. Finally, these data highlight the importance of accessory proteins in the regulation and modulation of ion channels. Further studies will be necessary to identify these accessory proteins.

Acknowledgements

The authors wish to thank Drs. Jim Melvin, Matthew Betzenhauser, Larry Wagner, Ted Begenisich, and Trevor Shuttleworth for helpful discussion during the course of this study and Lyndee Bilodeau and Jennifer Wintermute for their excellent technical assistance. Grants from the National Institutes of Health to D. I. Yule (DE14756) supported this study. During a portion of this study, D. A. Brown was supported by the National Institute of Dental and Craniofacial Research Training Grant T32-DE-07202.

Appendix A. Supplementary data

Supplementary data associated with this article can be found, in the online version, at doi:10.1016/j.bbamcr.2009.12.002.

References

[1] E.M. Schwiebert, A. Zsembery, Extracellular ATP as a signaling molecule for epithelial cells, Biochim. Biophys. Acta 1615 (2003) 7–32.
[2] R.A. North, Molecular physiology of P2X receptors, Physiol. Rev. 82 (2002) 1013–1067.
[3] J.T. Turner, L.A. Landon, S.J. Gibbons, B.R. Talamo, Salivary gland P2 nucleotide receptors, Crit. Rev. Oral Biol. Med. 10 (1999) 210–224.
[4] A.J. Brake, M.J. Wagenbach, D. Julius, New structural motif for ligand-gated ion channels defined by an ionotropic ATP receptor, Nature 371 (1994) 519–523.
[5] B.S. Khakh, R.A. North, P2X receptors as cell-surface ATP sensors in health and disease, Nature 442 (2006) 527–532.
[6] A. Nicke, H.G. Baumert, J. Rettinger, A. Eichele, G. Lambrecht, E. Mutschler, G. Schmalzing, P2X1 and P2X3 receptors form stable trimers: a novel structural motif of ligand-gated ion channels, Embo J. 17 (1998) 3016–3028.
[7] L.H. Jiang, M. Kim, V. Spelta, X. Bo, A. Surprenant, R.A. North, Subunit arrangement in P2X receptors, J. Neurosci. 23 (2003) 8903–8910.

[8] M.T. Young, P2X receptors: dawn of the post-structure era, Trends Biochem. Sci. (Oct 2009). PMID 19836961.
[9] T. Kawate, J.C. Michel, W.T. Birdsong, E. Gouaux, Crystal structure of the ATP-gated P2X(4) ion channel in the closed state, Nature 460 (2009) 592–598.
[10] T. Kawaguchi, S. Murai, H. Saito, T. Itoh, Changes in the noradrenaline and acetylcholine content of three major salivary glands and in the salivation and protein component patterns of whole saliva in chronically isoprenaline-administered mice, Arch. Oral Biol. 42 (1997) 225–234.
[11] K.T. Le, K. Babinski, P. Seguela, Central P2X4 and P2X6 channel subunits coassemble into a novel heteromeric ATP receptor, J. Neurosci. 18 (1998) 7152–7159.
[12] C. Lewis, S. Neidhart, C. Holy, R.A. North, G. Buell, A. Surprenant, Coexpression of P2X2 and P2X3 receptor subunits can account for ATP-gated currents in sensory neurons, Nature 377 (1995) 432–435.
[13] A. Nicke, D. Kerschensteiner, F. Soto, Biochemical and functional evidence for heteromeric assembly of P2X1 and P2X4 subunits, J. Neurochem. 92 (2005) 925–933.
[14] G.E. Torres, T.M. Egan, M.M. Voigt, Hetero-oligomeric assembly of P2X receptor subunits. Specificities exist with regard to possible partners, J. Biol. Chem. 274 (1999) 6653–6659.
[15] M. Paukert, R. Osteroth, H.S. Geisler, U. Brandle, E. Glowatzki, J.P. Ruppersberg, S. Grunder, Inflammatory mediators potentiate ATP-gated channels through the P2X(3) subunit, J. Biol. Chem. 276 (2001) 21077–21082.
[16] S.J. Ennion, R.J. Evans, P2X(1) receptor subunit contribution to gating revealed by a dominant negative PKC mutant, Biochem. Biophys. Res. Commun. 291 (2002) 611–616.
[17] E. Boue-Grabot, V. Archambault, P. Seguela, A protein kinase C site highly conserved in P2X subunits controls the desensitization kinetics of P2X(2) ATP-gated channels, J. Biol. Chem. 275 (2000) 10190–10195.
[18] Y.W. Chow, H.L. Wang, Functional modulation of P2X2 receptors by cyclic AMP-dependent protein kinase, J. Neurochem. 70 (1998) 2606–2612.
[19] D.A. Brown, J.I. Bruce, S.V. Straub, D.I. Yule, cAMP potentiates ATP-evoked calcium signaling in human parotid acinar cells, J. Biol. Chem. 279 (2004) 39485–39494.
[20] G. Kang, J.W. Joseph, O.G. Chepurny, M. Monaco, M.B. Wheeler, J.L. Bos, F. Schwede, H.G. Genieser, G.G. Holz, Epac-selective cAMP analog 8-pCPT-2′-O-Me-cAMP as a stimulus for Ca2+-induced Ca2+ release and exocytosis in pancreatic beta-cells, J. Biol. Chem. 278 (2003) 8279–8285.
[21] R. Kopperud, C. Krakstad, F. Selheim, S.O. Doskeland, cAMP effector mechanisms. Novel twists for an 'old' signaling system, FEBS Lett. 546 (2003) 121–126.
[22] D.A. Brown, D.I. Yule, Protein kinase C regulation of P2X3 receptors is unlikely to involve direct receptor phosphorylation, Biochim. Biophys. Acta 1773 (2007) 166–175.
[23] H. Sugawara, M. Kurosaki, M. Takata, T. Kurosaki, Genetic evidence for involvement of type 1, type 2 and type 3 inositol 1, 4, 5-trisphosphate receptors in signal transduction through the B-cell antigen receptor, Embo J. 16 (1997) 3078–3088.
[24] T. Miyakawa, A. Maeda, T. Yamazawa, K. Hirose, T. Kurosaki, M. Iino, Encoding of Ca2+ signals by differential expression of IP3 receptor subtypes, Embo J. 18 (1999) 1303–1308.
[25] H. Kubista, T. Hawkins, S.E. Moss, Characterisation of calcium signalling in DT40 chicken B-cells, Biochim. Biophys. Acta 1448 (1998) 299–310.
[26] L.E. Wagner II, W.H. Li, D.I. Yule, Phosphorylation of type-1 inositol 1, 4, 5-trisphosphate receptors by cyclic nucleotide-dependent protein kinases: a mutational analysis of the functionally important sites in the S2+ and S2− splice variants, J. Biol. Chem. 278 (2003) 45811–45817.
[27] L.E. Wagner II, W.H. Li, S.K. Joseph, D.I. Yule, Functional consequences of phosphomimetic mutations at key cAMP-dependent protein kinase phosphorylation sites in the type 1 inositol 1, 4, 5-trisphosphate receptor, J. Biol. Chem. 279 (2004) 46242–46252.
[28] D.A. Brown, J.E. Melvin, D.I. Yule, Critical role for NHE1 in intracellular pH regulation in pancreatic acinar cells, Am. J. Physiol. Gastrointest. Liver Physiol. 285 (2003) G804–G812.
[29] J.H. Won, D.I. Yule, Measurement of Ca2+ signaling dynamics in exocrine cells with total internal reflection microscopy, Am. J. Physiol. Gastrointest. Liver Physiol. 291 (2006) G146–G155.
[30] H.C. Cheng, B.E. Kemp, R.B. Pearson, A.J. Smith, L. Misconi, S.M. Van Patten, D.A. Walsh, A potent synthetic peptide inhibitor of the cAMP-dependent protein kinase, J. Biol. Chem. 261 (1986) 989–992.
[31] S.J. Royle, L.K. Bobanovic, R.D. Murrell-Lagnado, Identification of a non-canonical tyrosine-based endocytic motif in an ionotropic receptor, J. Biol. Chem. 277 (2002) 35378–35385.
[32] S.J. Royle, O.S. Qureshi, L.K. Bobanovic, P.R. Evans, D.J. Owen, R.D. Murrell-Lagnado, Non-canonical YXXGPhi endocytic motifs: recognition by AP2 and preferential utilization in P2X4 receptors, J. Cell Sci. 118 (2005) 3073–3080.
[33] L.K. Bobanovic, S.J. Royle, R.D. Murrell-Lagnado, P2X receptor trafficking in neurons is subunit specific, J. Neurosci. 22 (2002) 4814–4824.
[34] S.J. Ennion, R.J. Evans, Agonist-stimulated internalisation of the ligand-gated ion channel P2X(1) in rat vas deferens, FEBS Lett. 489 (2001) 154–158.
[35] J.S. Herskovits, C.C. Burgess, R.A. Obar, R.B. Vallee, Effects of mutant rat dynamin on endocytosis, J. Cell Biol. 122 (1993) 565–578.
[36] E. Toulme, F. Soto, M. Garret, E. Boue-Grabot, Functional properties of internalization-deficient P2X4 receptors reveal a novel mechanism of ligand-gated channel facilitation by ivermectin, Mol. Pharmacol. 69 (2006) 576–587.
[37] O. Olusanya, P.D. Andrews, J.R. Swedlow, E. Smythe, Phosphorylation of threonine 156 of the mu2 subunit of the AP2 complex is essential for endocytosis in vitro and in vivo, Curr. Biol. 11 (2001) 896–900.
[38] A. Wilde, F.M. Brodsky, In vivo phosphorylation of adaptors regulates their interaction with clathrin, J. Cell Biol. 135 (1996) 635–645.
[39] A. Priel, S.D. Silberberg, Mechanism of ivermectin facilitation of human P2X4 receptor channels, J. Gen. Physiol. 123 (2004) 281–293.
[40] C. Vial, A.B. Tobin, R.J. Evans, G-protein-coupled receptor regulation of P2X1 receptors does not involve direct channel phosphorylation, Biochem. J. 382 (2004) 101–110.
[41] W. Ma, A. Korngreen, S. Weil, E.B. Cohen, A. Priel, L. Kuzin, S.D. Silberberg, Pore properties and pharmacological features of the P2X receptor channel in airway ciliated cells, J. Physiol. 571 (2006) 503–517.
[42] K. Yamamoto, T. Sokabe, T. Matsumoto, K. Yoshimura, M. Shibata, N. Ohura, T. Fukuda, T. Sato, K. Sekine, S. Kato, M. Isshiki, T. Fujita, M. Kobayashi, K. Kawamura, H. Masuda, A. Kamiya, J. Ando, Impaired flow-dependent control of vascular tone and remodeling in P2X4-deficient mice, Nat. Med. 12 (2006) 133–137.